The Astronomical Journal, 128:1882–1893, 2004 October

CATACLYSMIC VARIABLES FROM THE SLOAN DIGITAL SKY SURVEY. III. THE THIRD YEAR[1]

Paula Szkody,[2] Arne Henden,[3,4] Oliver Fraser,[2] Nicole Silvestri,[2] John Bochanski,[2] Michael A. Wolfe,[2] Marcel Agüeros,[2] Brian Warner,[5] Patrick Woudt,[5] Jonica Tramposch,[2] Lee Homer,[2] Gary Schmidt,[6] Gillian R. Knapp,[7] Scott F. Anderson,[2] Kevin Covey,[2] Hugh Harris,[3] Suzanne Hawley,[2] Donald P. Schneider,[8] Wolfgang Voges,[9] and J. Brinkmann[10]

Received 2004 April 12; accepted 2004 July 8

ABSTRACT

This paper continues the series that identifies new cataclysmic variables found in the Sloan Digital Sky Survey (SDSS). We present 36 cataclysmic variables and one possible symbiotic star from Sloan spectra obtained during 2002, of which 34 are new discoveries, two are known dwarf novae (BC UMa and KS UMa), and one is a known cataclysmic variable identified from the Two-Degree Field survey. The positions, colors, and spectra of all 37 systems are presented, along with follow-up spectroscopic/photometric observations of 10 systems. As in the past 2 yr of data, the new SDSS systems show a large variety of characteristics based on their inclination and magnetic fields, including three eclipsing systems, four with prominent He II emission, and 15 systems showing features of the underlying stars.

Key words: binaries: eclipsing — binaries: spectroscopic — novae, cataclysmic variables — stars: dwarf novae

1. INTRODUCTION

At the present time, the Sloan Digital Sky Survey (SDSS) data have been released to the public as the Early Data Release (EDR; Stoughton et al. 2002), Data Release 1 (DR1; Abazajian et al. 2003),[11] and Data Release 2 (DR2; Abazajian et al. 2004). Mining the database for cataclysmic variables (CVs) has resulted in the discovery of 19 new CVs from the SDSS spectra obtained through 2000 December 31 (Szkody et al. 2002, hereafter Paper I) and an additional 35 from spectra through 2001 December 31 (Szkody et al. 2003b, hereafter Paper II). This paper continues the series that is reporting CVs on a yearly basis with 36 systems (and one possible symbiotic star) that were found among the SDSS spectra obtained during the year 2002. Three of these objects were previously known from past X-ray or optical surveys, whereas the rest are new discoveries. Follow-up photometric and spectroscopic observations of the new systems, providing light and radial velocity curves, can allow a determination of their orbital period, which is a fundamental parameter in identifying CVs. (See Warner 1995 for a comprehensive review of all types of CVs.)

2. OBSERVATIONS AND REDUCTIONS

The details of the SDSS imaging and spectroscopic instrumentation and reductions are explained in Paper I and in the papers by Fukugita et al. (1996), Gunn et al. (1998), Lupton et al. (1999, 2001), York et al. (2000), Hogg et al. (2001), Smith et al. (2002), and Pier et al. (2003). Briefly, SDSS photometry in five filters (*u*, *g*, *r*, *i*, and *z*) is used to select objects by color for later spectroscopy in the range of 3900–6200 Å (blue beam) and 5800–9200 Å (red beam) at a resolving power of ~1800. The spectra are calibrated for wavelength and flux and then classified as stars, galaxies, and quasars. As explained in Papers I and II, cataclysmic variables have spectra obtained through several color selection algorithms, since their colors overlap with those of hot stars, quasars, white dwarfs, and M stars, depending on how much the accretion disk or accretion column contributes to the optical light over that of the underlying white dwarf and late-type secondary star. The only difference in the procedures used in this paper over those in the past two papers is that we have automated the identification process with a computer script that finds all spectra with Balmer absorption or emission lines on a given plate (instead of inspecting all spectra on a plate by hand). The resulting spectra are then hand-identified as white dwarfs or CVs. As a cross-check on the accuracy of the computer identification, all the DR1 plates were run through the algorithm, and all the previous CVs identified in Papers I and II were recovered.

The list of 36 CVs (and the possible symbiotic) found in SDSS spectra taken in 2002 is presented in Table 1. As in the previous listings, the magnitudes and colors are from the point-spread function photometry with no correction for interstellar reddening. To make it easier to locate objects in the spectral database, we give the plate, fiber, and MJD of each spectrum in the Table. For convenience, we refer to these objects throughout the rest of this paper as SDSSJ *hhmm* (where *hhmm* is the right ascension in hours and minutes), except for two objects which have identical R. A. coordinates, so we add the first two digits of declination to discriminate.

[1] Based on observations obtained with the Sloan Digital Sky Survey and with the Apache Point Observatory (APO) 3.5 m telescope, which are owned and operated by the Astrophysical Research Consortium.

[2] Department of Astronomy, University of Washington, Box 351580, Seattle, WA 98195.

[3] US Naval Observatory, Flagstaff Station, P.O. Box 1149, Flagstaff, AZ 86002.

[4] Universities Space Research Association.

[5] Department of Astronomy, University of Cape Town, Rondebosch 7700, South Africa.

[6] Steward Observatory, University of Arizona, Tucson, AZ 85721.

[7] Princeton University Observatory, Princeton, NJ 08544.

[8] Department of Astronomy and Astrophysics, 525 Davey Laboratory, Pennsylvania State University, University Park, PA 16802.

[9] Max-Planck-Institut für extraterrestrische Physik, Geissenbachstrasse 1, D-85741 Garching, Germany.

[10] Apache Point Observatory, P.O. Box 59, Sunspot, NM 88349.

[11] See http://www.sdss.org.

TABLE 1
SUMMARY OF CVs WITH SDSS SPECTRA IN 2002[a]

SDSSJ	MJD-P-F[b]	g	$u-g$	$g-r$	$r-i$	$i-z$	P[c] (hr)	Comments[d]
004335.14−003729.8	52531-1085-175	19.84	0.37	0.01	−0.23	0.18	1.3:	
074813.54+290509.2[e]	52618-1059-407	18.62	−0.08	−0.16	0.01	−0.05	2.5:	He II NP
080846.19+313106.0*	52318-861-352	19.43	−0.29	0.68	0.62	0.40		DN
090016.56+430118.2*	52294-831-435	18.88	−0.22	0.68	0.69	0.49	5.3:	
090403.48+035501.2*	52238-566-380	19.24	0.26	−0.09	−0.18	0.04	1.4	ec
090452.09+440255.4*	52294-831-410	19.38	0.29	−0.11	−0.23	−0.07		
093249.57+472523.0*	52316-834-431	17.81	0.22	−0.03	−0.08	0.05	1.7:	He II
094325.90+520128.8*	52281-768-13	16.45	0.15	−0.10	−0.15	−0.16		
095135.21+602939.6*	52282-770-358	20.02	−0.12	0.03	−0.21	0.16		
101323.64+455858.9	52614-944-397	18.86	−0.33	−0.03	0.15	0.29		
102026.53+530433.1*	52381-904-147	17.44	−0.08	0.24	−0.04	0.28	1.6	KS UMa
113215.50+624900.4*	52319-776-381	18.49	−0.30	0.16	0.08	−0.06		
115215.83+491441.9	52412-968-280	18.51	0.14	−0.10	−0.09	0.31	1.5	BC UMa
115639.48+630907.7*	52320-777-574	20.73	0.38	1.79	0.22	−0.04		
121607.03+052013.9*	52378-844-423	20.12	0.21	0.12	−0.29	0.00		
124426.26+613514.6*	52373-781-93	18.76	−0.04	−0.11	0.07	0.35		
124959.76+035726.6*	52426-847-46	16.63	−0.35	−0.05	0.38	0.28		
130236.21+060148.0*	52439-849-419	21.59	2.33	1.62	2.26	1.25		symb-like
130514.73+582856.3*	52410-958-297	19.27	−0.17	−0.04	0.19	0.05		
132411.57+032050.5*	52342-527-323	22.12	1.21	1.63	0.26	0.79	2.6	Polar
133540.76+050722.7*	52374-853-498	18.46	−0.02	−0.17	−0.16	−0.20		
142256.31−022108.1*	52404-918-301	19.84	−0.35	0.50	0.36	0.27		2dF, He II
150137.22+550123.4*	52353-792-44	19.40	0.24	0.02	−0.21	0.01	1.3	ec
153817.35+512338.0*	52401-796-388	18.61	−0.23	−0.28	−0.14	0.21	1.6:	
155037.27+405440.0*	52468-1053-14	18.58	−0.34	0.21	0.11	−0.17		
161030.35+445901.7*	52443-814-280	19.81	0.08	−0.06	−0.47	0.14		
162212.45+341147.3	52522-1057-203	19.15	0.19	0.43	0.30	0.40		He II
162608.16+332827.8	52520-1058-433	18.38	0.08	−0.21	−0.21	−0.07		He II
170213.26+322954.1*	52426-973-144	17.92	−0.60	0.10	0.40	0.60	2.5	ec
170324.09+320953.2*	52426-973-97	18.17	−0.77	0.56	0.36	0.56		
170542.54+313240.8*	52411-975-400	19.67	0.12	0.48	0.48	0.25		
171145.08+301320.0*	52410-977-402	20.25	0.20	0.05	−0.09	−0.09		
204720.76+000007.7*	52466-982-477	19.40	−0.12	0.15	0.02	0.02		
210014.12+004446.0*	52442-984-533	18.78	−0.19	0.10	0.07	0.03	1.9	DN
210241.09−004408.3*	52438-984-52	17.22	1.29	0.10	0.07	0.02		
211605.43+113407.5*	52468-729-363	15.31	0.04	−0.26	−0.16	−0.20		
223252.35+140353.0	52521-738-509	17.69	0.14	−0.15	−0.08	−0.09		DN

[a] Objects marked with asterisk are publicly available in the SDSS DR2.
[b] Last 5 digits of Modified Julian Date of spectrum-plate-fiber.
[c] Periods marked with a colon are estimates based on single-night observations.
[d] DN is a dwarf nova, ec is eclipsing, NP is not polarized, symb is symbiotic.
[e] Object is the southeastern star of a close pair.

We were able to conduct follow-up observations on several systems to refine their characteristics (predominantly an estimate of their orbital period and whether they were at a high enough inclination to be eclipsing). Photometry was accomplished with the US Naval Observatory Flagstaff Station (NOFS) 1 m telescope with a 1024×1024 SITe/Tektronix CCD. Differential photometry with respect to stars in the field was used to obtain light curves. With one exception, no filter was used to maximize the signal-to-noise ratio (S/N), but nights of calibrated all-sky photometry with Landolt standards were used to calibrate the comparison stars so that the photometry could be placed onto the Johnson V magnitude system. For the brightest system (SDSSJ 0808), a V filter was used for the observation.

Time-resolved spectroscopy was accomplished at the Apache Point Observatory (APO) 3.5 m telescope with the Double Imaging Spectrograph in high-resolution mode (resolution about 3 Å) and a 1.″5 slit. The reductions were identical to those of Papers I and II. Velocities were measured with either the "e" (which determines the centroid of the line) or "k" (which fits a Gaussian to the line) in the IRAF[12] SPLOT package (for simple or narrow-line structure) or with a double-Gaussian method (Shafter 1983) for lines with central absorption or narrow emission components within the broad emission. Least-squares fitting of sinusoids to the velocities was then performed to determine γ (systemic velocity), K (semi-amplitude), P (orbital period), and ϕ_0 (phase of crossing from redshift to blueshift). Note that since the spectroscopic solutions from APO data are based on a single night of data, the periods are only estimates that need to be fully determined with

[12] IRAF (the Image Reduction and Analysis Facility) is distributed by the National Optical Astronomy Observatory, which is operated by the Association of Universities for Research in Astronomy, Inc., under cooperative agreement with the National Science Foundation.

TABLE 2
Follow-up Data

SDSSJ	UT Date	Site	Time (UT)	Exposure (s)	Data Obtained
0043.....	2003 Sep 27	APO	06:22–09:05	900	10 spectra
0748.....	2003 Sep 27	APO	09:28–12:04	600/900	10 spectra
0748.....	2003 Nov 1	MMT	09:52–10:32	2400	Spectropolarimetry
0748.....	2004 Jan 28	NOFS	02:04–06:16	180	Photometry
0808.....	2003 Nov 27	APO	09:04–09:24	1200	1 spectrum
0808.....	2004 Jan 26	NOFS	03:04–12:10	90	V photometry
0900.....	2002 Feb 22	APO	02:41–06:41	600	21 spectra
0900.....	2004 Jan 29	NOFS	02:14–11:44	180	Photometry
0932.....	2002 Jan 4	APO	05:38–09:26	900	14 spectra
1501.....	2003 Jun 25	NOFS	04:05–09:22	240	Photometry
1538.....	2002 Jun 26	APO	04:54–06:40	900/600	9 spectra
1702.....	2002 Oct 3	APO	02:29–03:29	600	6 spectra
1702.....	2003 Apr 27	APO	10:37–11:34	600/900	4 spectra
1702.....	2003 Jun 26	APO	06:52–10:10	600	16 spectra
1702.....	2003 Jul 3	NOFS	03:34–10:48	180	Photometry
2102.....	2003 Dec 21	APO	01:19–02:14	600	5 spectra
2232.....	2003 Oct 20	NOFS	01:33–08:34	240	Photometry

longer data sets. The estimates are designated in Table 1 with a colon following the period.

Circular polarization measurements were obtained for SDSSJ 0748, using the CCD Imaging/Spectropolarimeter with a low-resolution grating on the 6.5 m MMT at Mount Hopkins. The dates and types of follow-up observations are summarized in Table 2.

3. RESULTS

Figure 1 shows the SDSS spectra for all 37 systems, while Table 3 lists the equivalent widths and fluxes of the prominent hydrogen Balmer and helium emission lines. Using the appearance of the spectra and the follow-up data when available, we can separate the objects into various categories as described below.

3.1. *Previously Known Systems*

As SDSS makes no attempt to screen out previously known sources in the selection for objects that will receive fibers, known CVs are observed, as well as new systems. In 2002, the spectra of the known dwarf novae BC UMa (SDSSJ 1152) and KS UMa (SDSSJ 1020), as well at that of the Two-Degree Field (2dF) source (SDSSJ 1422) = 2QZ J142256.3−022108 (Croom et al. 2001) were obtained. Information on all three sources is available from the online CV catalog of R. Downes.[13] The detailed characteristics of SDSSJ 1324 as an unusual low accretion rate polar have already been published by Szkody et al. (2003a).

The SDSS spectrum of KS UMa was obtained during an outburst so it shows a typical disk-dominated spectrum. A spectrum of KS UMa at quiescence is shown by Jiang et al. (2000). BC UMa shows the broad absorption features surrounding the emission that is indicative of the prominence of the white dwarf (as previously noted by Mukai et al. 1990). SDSSJ 1422, on the other hand, has prominent He II emission and is a likely candidate for a system containing a magnetic white dwarf.

[13] Available at http://icarus.stsci.edu/~downes/cvcat/.

3.2. *High-Inclination Systems*

Generally, high-inclination CVs have very prominent central absorption in the Balmer lines (giving a double-peaked appearance), with increasing absorption up the Balmer series. Figure 1 shows that SDSSJ 0904, 1501, and 1702 are good candidates for high-inclination, eclipsing systems. Follow-up data on these three systems have confirmed that all three eclipse. SDSSJ 0904+03 shows a partial eclipse with a period of 86 minutes and will be discussed in detail in a separate paper (Woudt et al. 2004).

Photometry of SDSSJ 1501 (Fig. 2) reveals deep (>1.6 mag) eclipses with a period of 78 minutes. Note from Figure 2 that the 4 minute sampling does not resolve the eclipses very well, since they are of very short duration (<15 minutes). The light curve is relatively flat between eclipses, indicating the lack of a prominent hot spot where the mass transfer stream impacts the disk.

The light curve of SDSSJ 1702 (Fig. 3) is particularly interesting. It shows deep (1.5 mag) eclipses with a period of 2.5 hr, a secondary eclipse of 0.2 mag depth at phase 0.5, and a large (0.2 mag) hump preceding eclipse, which is likely the hot spot coming into view. Using the double-Gaussian method on the emission-line wings and fixing the period at 2.5 hr gives the radial velocity solutions listed in Table 4. Figure 4 shows the best fits to the Hα and Hβ lines. Note that the points near phase 0.9 (which are not included in the fit) show the usual large displacement to positive then to negative velocity that is typical for accretion disks undergoing an eclipse. SDSSJ 1702 is an excellent candidate for further follow-up observations with a large telescope; better time resolution for the light curve should be able to resolve the eclipse structure, which may show the white dwarf ingress and egress. The width of the eclipse combined with the radial velocity curve may provide an estimate of the white dwarf mass. In addition, Figure 1 shows that the M star is visible. Matching the TiO λ7050 band to the spectral index defined by Reid et al. (1995) for M stars yields a spectral type of M1.5 $\pm$ 1.1. Then, using the absolute magnitude versus spectral type relations from Hawley et al. (2002) with the i and z magnitudes listed in Table 1 yields a distance of 610 pc from the i magnitude, 580 pc

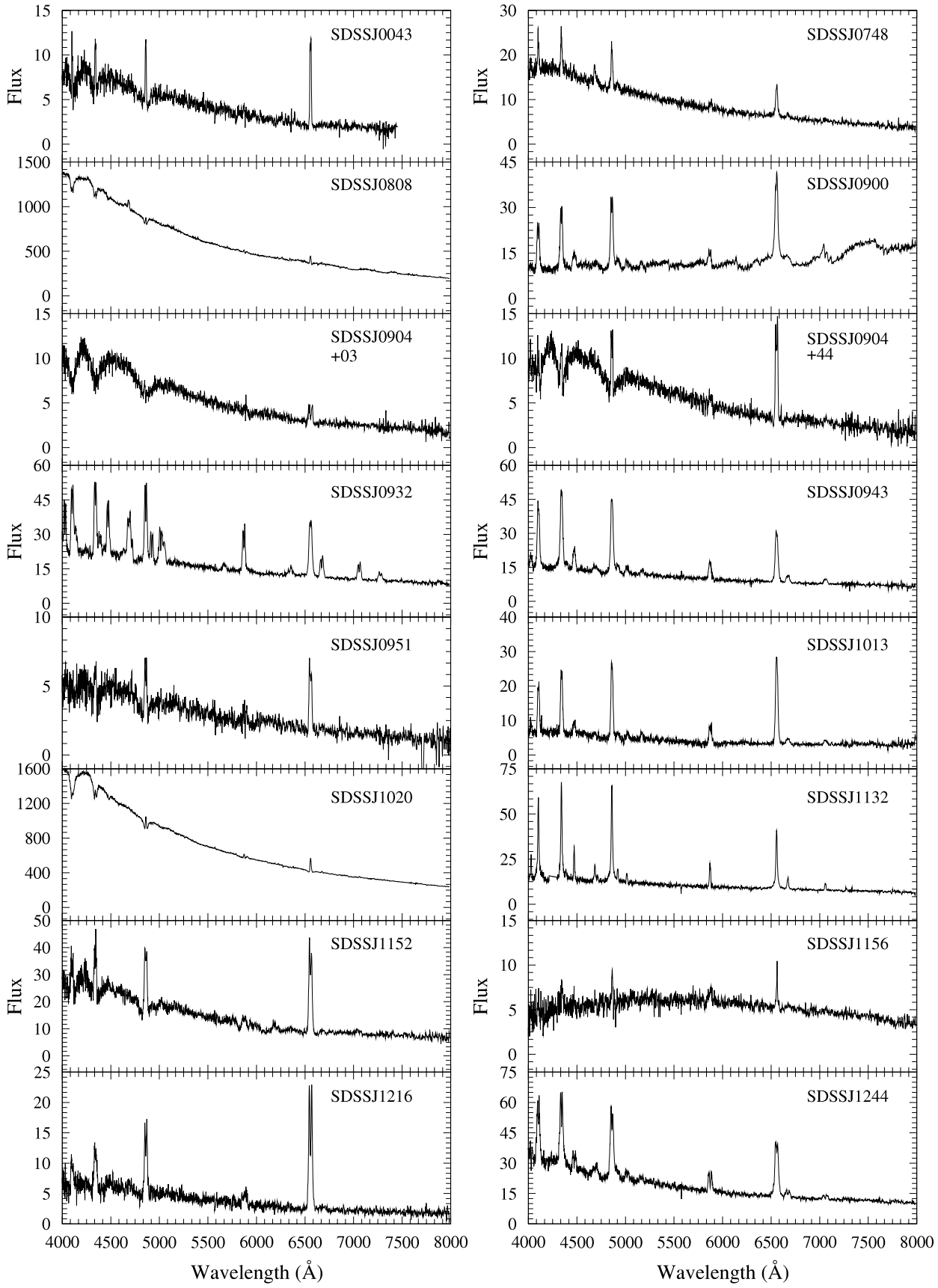

FIG. 1.—SDSS spectra of the 36 CVs and one possible symbiotic. The flux scale is in units of flux density 10^{-17} ergs cm^{-2} s^{-1} Å^{-1}. The spectral resolution is about 3 Å.

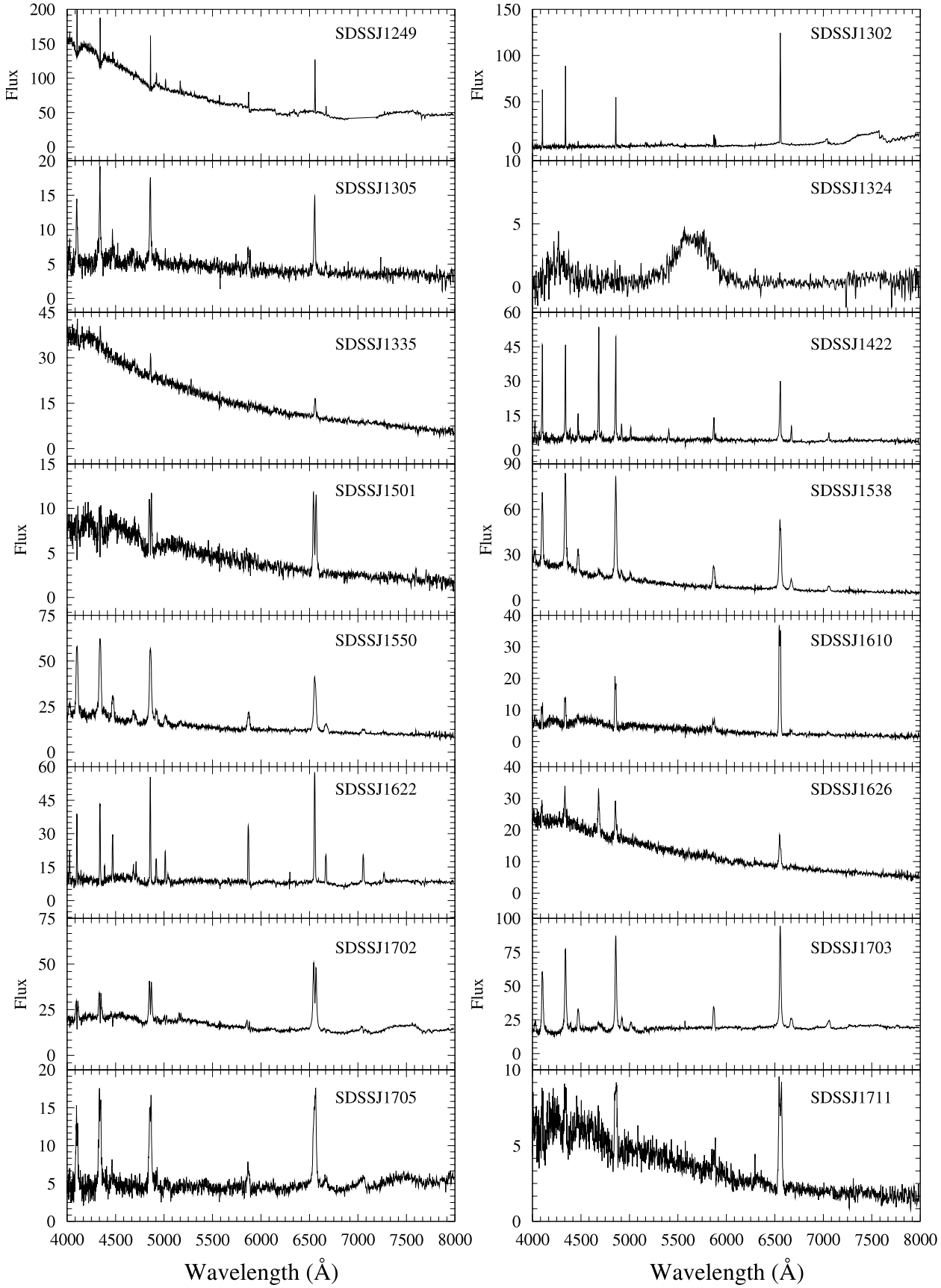

FIG. 1.—*Continued*

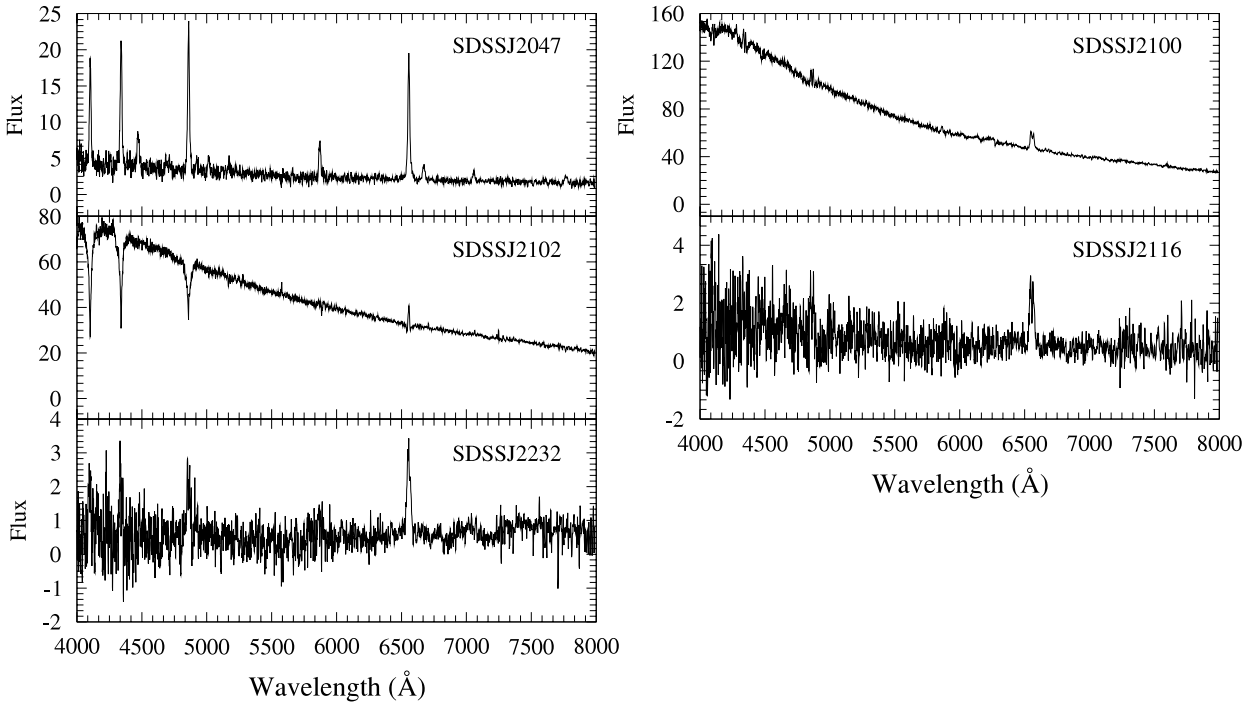

FIG. 1.—*Continued*

from the z magnitude, and 570 pc using the J magnitude from the Two Micron All Sky Survey database ($J = 15.63 \pm 0.05$). With the uncertainties in the spectral type, the total range of distances allowed is between 460 and 650 pc.

An attempt was made to determine the velocity of the M dwarf by using the IRAF routine FXCOR to cross-correlate the red spectra against the one in eclipse, but the individual spectra were too noisy to derive a believable result. Time-resolved, higher S/N data should be able to determine the velocity curve of the secondary, thus leading to a good determination of the mass ratio. SDSSJ 1702 is potentially very useful, as it is one of the very few double-lined, eclipsing CVs from which masses can be found. A mass measurement for this system would be particularly interesting, as its period is squarely in the period gap (a region between 2 and 3 hr that is rarely occupied by dwarf novae). SDSSJ 1702 can provide a good test of the evolution models of Howell et al. (2001), which make predictions for the masses above and below the gap.

3.3. *Dwarf Novae*

The SDSS spectrum of SDSSJ 0808 was obtained during a likely dwarf nova outburst and is similar to the SDSS outburst spectrum of KS UMa (SDSSJ 1020). Both the SDSS image and the Digitized Sky Survey (DSS) show SDSSJ 0808 as a fainter object than implied by the spectrum in Figure 1. An APO spectrum obtained on 2003 November 27 (Fig. 5) shows the typical strong emission lines of a quiescent dwarf nova. It is likely that this object has fairly frequent outbursts, as follow-up photometry at USNO also caught SDSSJ 0808 during outburst (at $V = 14.5$). The outbursts are fairly long, as an observation a week after the first one showed the system still at 14.7. The 9 hr of observation at that time (Fig. 6) show a modulation with amplitude of 0.04 mag on a timescale of 6 hr superposed on a declining brightness trend throughout the observation. However, since it is usually not possible to determine an orbital period from outburst photometry and a radial velocity curve is not yet available, further data will be needed to determine whether the 6 hr timescale is related to the orbital period of this system or merely transient fluctuations in the mass accretion as the system returned to quiescence.

The SDSS spectrum of SDSSJ 2100 (Fig. 1) also looks similar to an outbursting dwarf nova, and the SDSS image and photometry (Table 1) are fainter as well. Optical photometry over several nights and during different accretion states revealed a large amplitude (0.2–0.5 mag) periodic modulation at 1.9 hr (or a possible alias at 2.1 hr); the detailed results are discussed in a separate paper (Tramposch et al. 2004).

SDSSJ 2232 was found in outburst during the SDSS imaging (Table 1) while it was in quiescence during the SDSS spectrum (Fig. 1). USNO photometry during quiescence on 2003 January 8 and 12 showed $V = 22.4$ and $B = 22.8 \pm 0.5$ mag, while an outburst ($V = 18.45$) was caught on 2003 October 20 (Table 2). The time series during outburst did not reveal any modulation.

Lastly, SDSSJ 2102 has the appearance of a dwarf nova during outburst, but with exceptionally strong Balmer absorption. Additional spectra obtained at APO in 2003 December showed a similar appearance, and the SDSS and DSS images show comparable brightness. Thus, it is more likely that this is a system with a prominent white dwarf. It is possible that this could be a detached system, although Hα is broader than a typical line caused by irradiation of the secondary by the white dwarf. Time-resolved spectroscopy can reveal if this is a long-period, widely separated binary.

3.4. *Nova-like Variables with Strong* He II

Strong He II emission lines usually indicate either a magnetic white dwarf, where the EUV continuum from an accretion

TABLE 3

SDSS Emission-Line Fluxes and Equivalent Widths[a]

	Hβ		Hα		He λ4471		He II 4686	
SDSSJ	*F*	EW	*F*	EW	*F*	EW	*F*	EW
0043.....	1	23	1.8	91	...	...	...	...
0748.....	1.7	13	1.7	27	0.12	1	0.5	4
0808.....	5.9	1	...	...	8.4	1	...	...
0900.....	6.9	61	10	75	1.1	10	...	...
0904+03	0.2	3.0	0.7	26	...	...	...	...
0904+44	1.4	23	2.9	93	...	...	...	...
0932.....	8.9	43	9.2	74	5.3	23	5.8	26
0943.....	8.9	60	7.8	87	2.3	15	0.6	4
0951.....	1.2	46	1.6	89	...	...	...	...
1013.....	5.4	96	7.0	176	0.8	12	...	...
1020.....	16	2	19	5	...	...	...	...
1132.....	9.9	70	6.7	71	2.0	13	1.3	10
1152.....	7.4	46	11.3	127	0.4	2	...	...
1156.....	0.5	9	0.6	12	...	...	...	...
1216.....	3.6	73	7.0	245	...	...	...	...
1244.....	14.9	64	12.4	92	2.4	9	1.4	6
1249.....	2.5	3	4.3	8	...	...	...	...
1302.....	2.5	104	8.9	153	0.3	18	...	...
1305.....	2.1	38	2.0	51	0.5	8	0.1	2
1335.....	0.6	2	0.9	8	...	...	...	...
1422.....	4.6	97	3.5	73	1.0	19	3.9	63
1501.....	1.6	33	2.9	101	...	...	...	...
1538.....	13.5	84	12.7	167	2.4	12	0.8	5
1550.....	9.5	49	9.3	79	3.5	19	1.6	9
1610.....	2.0	53	5.5	320	...	...	...	...
1622.....	4.8	57	6.3	73	1.8	17	0.6	6
1626.....	2	11	1.9	22	...	...	1.9	10
1702.....	6.4	33	13.1	88	...	...	...	...
1703.....	11.6	56	14.7	73	3.1	17	1.3	7
1705.....	3.8	83	4.4	90	0.4	7	...	...
1711.....	1.3	31	2.4	97	...	...	...	...
2047.....	3.5	102	3.6	173	1.1	30	0.2	6
2100.....	0.4	2	0.9	8	...	...	...	...
2102.....	...	...	1.2	4	...	...	...	...
2116.....	0.4	38	0.8	143	...	...	...	...
2232.....	0.7	187	0.9	167	...	...	...	...

[a] Fluxes are in units of 10^{-15} ergs cm^{-2} s^{-1}; equivalent widths are in units of angstroms.

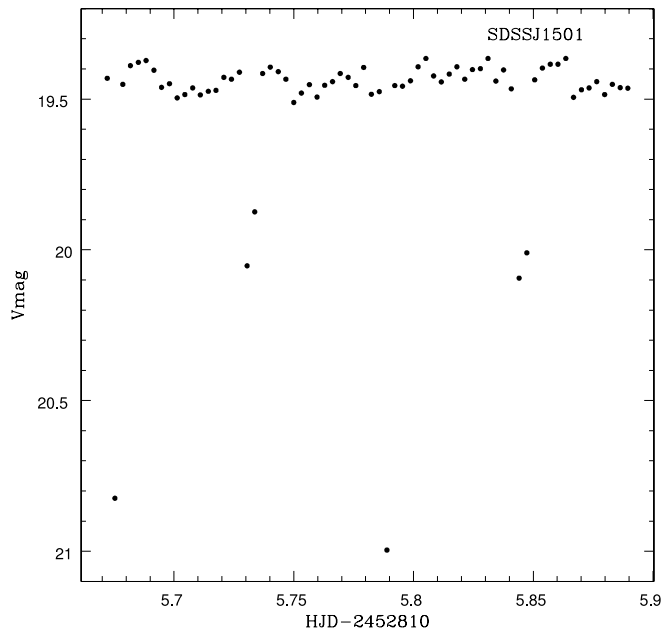

FIG. 2.—NOFS light curve of SDSSJ 1501. Integration times are 4 minutes, and photometric errors are 0.04 mag on each point except during eclipses.

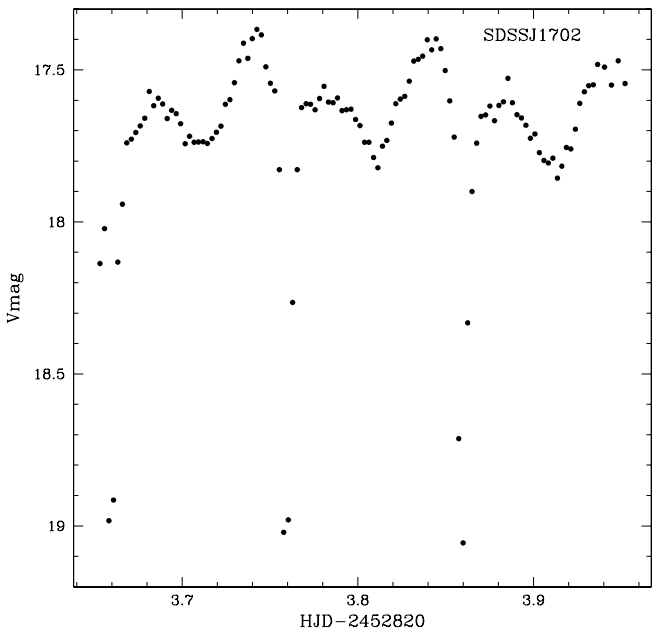

FIG. 3.—NOFS light curve of SDSSJ 1702. Integrations are 3 minutes, with errors of 0.01 mag outside of eclipse.

TABLE 4
RADIAL VELOCITY SOLUTIONS

SDSSJ	Line	P (hr)	γ	K (km s^{-1})	T_0 (JD 2,452,000+)	σ
0043.....	Hα	1.5	17 ± 1	68 ± 16	909.830	28
0043.....	Hβ	1.2	-0.7 ± 1.3	90 ± 12	909.783	27
0748.....	Hα	2.5	-32 ± 1	177 ± 23	909.965	42
0748.....	Hβ	2.5	-82 ± 1	157 ± 45	909.958	85
0900.....	Hα	4.7	54 ± 7	168 ± 14	327.706	36
0900.....	Hβ	5.3	89 ± 9	140 ± 14	327.707	39
0900.....	Hγ	4.5	77 ± 2	126 ± 12	327.707	38
0932.....	Hα	1.7	-2 ± 2	109 ± 25	278.752	61
0932.....	Hβ	1.7	-99 ± 5	168 ± 30	278.755	76
0932.....	Hγ	1.6	-14 ± 6	169 ± 33	278.755	83
1538.....	Hα	1.7	-19 ± 1	103 ± 4	451.744	9
1538.....	Hβ	1.5	25 ± 1	160 ± 12	451.743	24
1538.....	Hγ	1.6	-87 ± 2	106 ± 6	451.748	11
1702.....	Hα	2.5	-26 ± 4	110 ± 10	451.855	23
1702.....	Hβ	2.5	51 ± 5	124 ± 13	451.856	31

shock ionizes the plasma, or a nova-like system with a high level of mass transfer, often a type of system called an SW Sextantis star. These types are ultimately differentiated by polarimetry, although time-resolved photometry and spectroscopy can yield distinct clues. An object that has a large circular polarization and a strong modulation of the lines and continuum at the orbital period is classified as a spin-orbit synchronized AM Herculis system, or polar. (See the review of polars in Wickramasinghe & Ferrario 2000.) One that has little or no polarization and is observed to have a periodicity at a spin timescale of the white dwarf (minutes) is considered an intermediate polar (IP), while one with an orbital period between 3 and 4 hr and single-peaked emission lines is likely an SW Sextantis star. (See Warner 1995 for a review of all types.)

The systems SDSSJ 0748, 0932, 1422, and 1626 clearly show He II. Of these, SDSSJ 1422 (the 2dF source) and SDSSJ 1626 are the best candidates for polars, as they have He II greater than Hβ. Spectropolarimetry was accomplished for SDSSJ 0748, but no polarization was seen to a level of 0.04%, so a polar nature is ruled out for this object. Spectroscopy suggests that the orbital period could be on the order of 2.5 hr (Fig. 7 and Table 4), but the data set is only 2.6 hr long, so further spectroscopy is needed for a correct determination. While He II emission was present in the APO spectra, the poor S/N due to high air mass at the time of observations prevented any determination of the velocities or period from the lines in the blue portion of the spectrum. Because of the proximity of a close companion on the sky, the

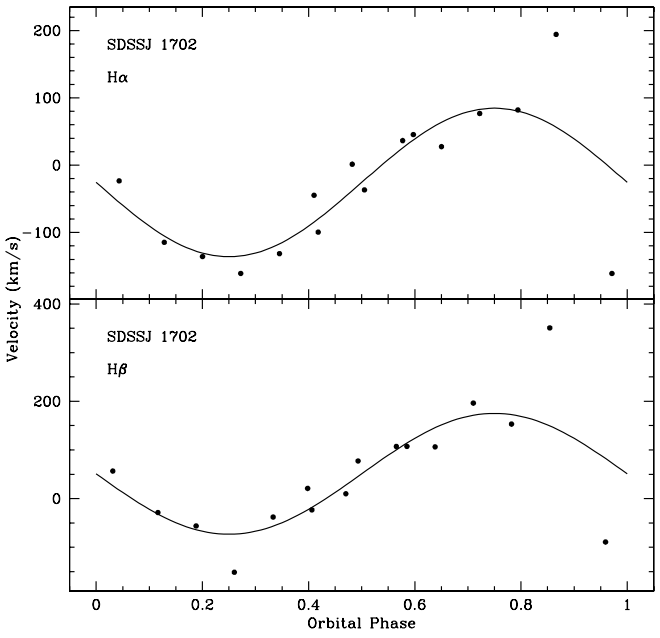

FIG. 4.—Velocity curves of SDSSJ 1702 with the best-fit sinusoids (Table 4) plotted on the data. The two discrepant points near phase 1 are not included in the sine fit.

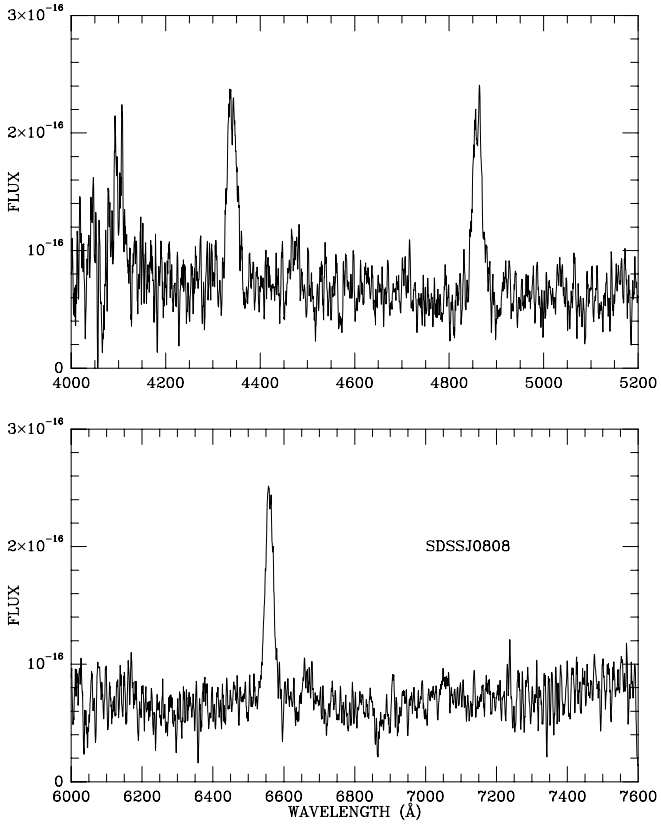

FIG. 5.—APO quiescent spectra of SDSS J0808 obtained 2003 November 27.

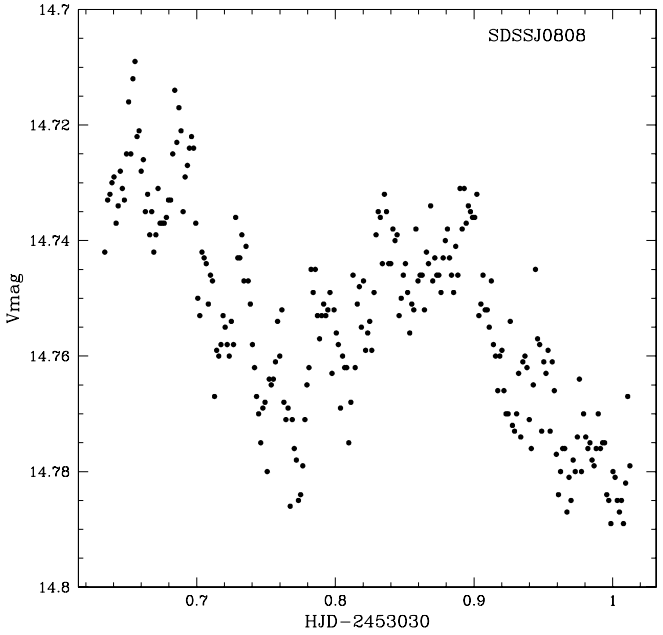

FIG. 6.—NOFS light curve of SDSSJ 0808 obtained near outburst in a *V* filter. Integration times are 1.5 minutes, and photometric errors are 0.004 mag.

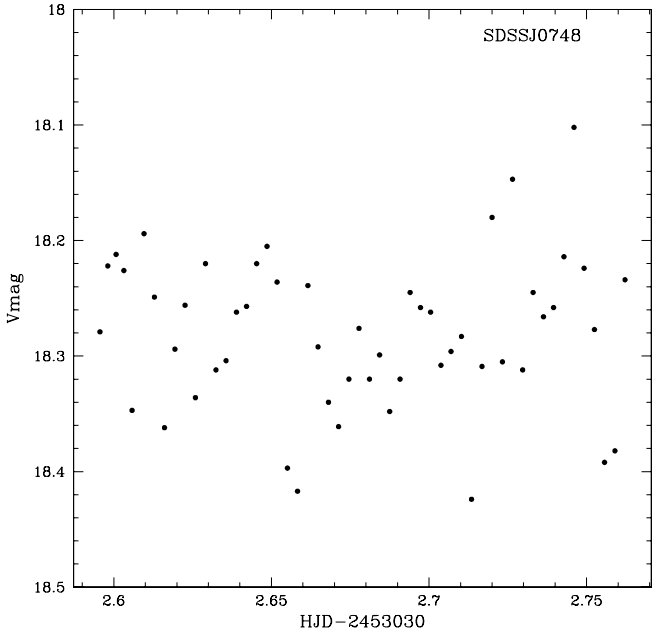

FIG. 8.—NOFS light curve of SDSSJ 0748. Each point is a 3 minute integration with error bar of 0.03. The aperture used included both the object and a close (fainter) companion on the sky.

photometry of this object was accomplished with an aperture that included both stars. The light curve (Fig. 8) shows no clear modulation at the 2.5 hr period. However, the PDM (epoch-folding) period search method available in IRAF reveals a prominent minimum at a period of 70 minutes. Since the light curve is only 4 hr long, further photometric data are also needed to determine whether this is merely active flickering or a stable period that could be identified with the spin of the white dwarf (which would indicate this system could be an IP).

SDSSJ 0932: This object was discovered as US 691 in the Usher survey of faint blue objects at high Galactic latitude (Usher et al. 1982). Its spectrum is very unusual in that it shows very strong doubled helium emission lines as well as the Balmer hydrogen lines. This doubling implies an origin in a disk. Neither polars nor SW Sextantis stars show this behavior. The unusual strength and structure in the He lines in SDSSJ 0932 is reminiscent of the SDSS-discovered CV SDSSJ 102347.67+003841.2 (Bond et al. 2002; Szkody et al. 2003b). It is not clear why these two systems have such strong and doubled He lines in comparison with normal nova-likes. While SDSSJ 1023 is a FIRST radio source, implying a magnetic nature, there is no radio source within 30″ of SDSSJ 0932. However, observations have shown that these radio sources can be highly variable (P. Mason 2004, private communication).

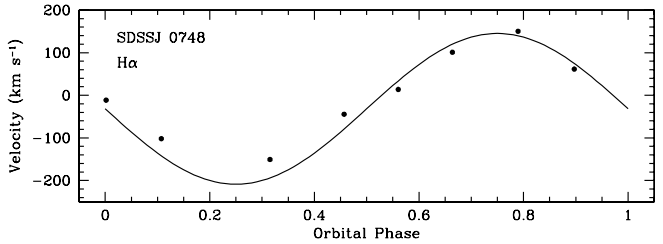

FIG. 7.—Hα velocity curve of SDSSJ 0748 with the best-fit sinusoid from Table 4.

Our radial velocity data (Fig. 9 and Table 4) give a best fit to a sine curve suggesting a period near 1.7 hr, but the overall errors are large for the brightness level of this system, so further data are definitely needed. It would be useful to obtain a longer set of time-resolved spectra with higher time resolution in order to construct tomograms that could help to locate the He II emission. Usually, this line is produced close to the white dwarf and provides the best velocity measurement value for the white dwarf. If the inner disk is disrupted, the line may originate further out in the disk (giving a doubled appearance) but must still be close enough to receive the excitation provided by high-energy photons.

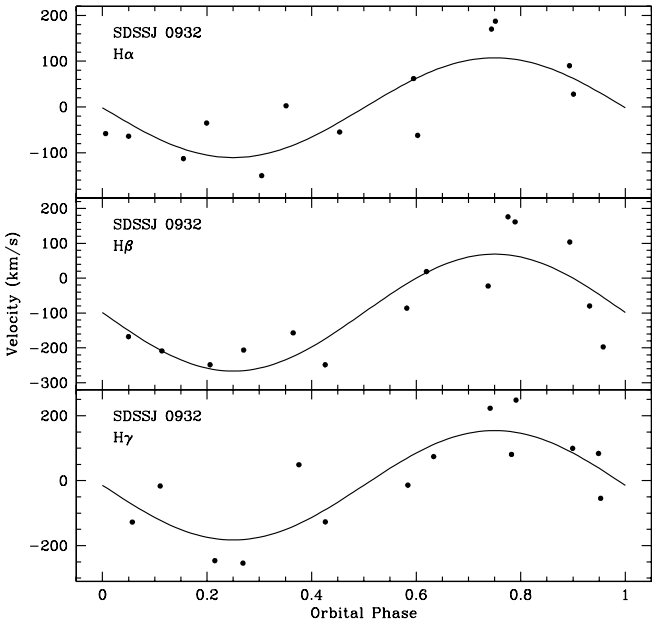

FIG. 9.—Velocity curves of SDSSJ 0932 with the best-fit sinusoids from Table 4.

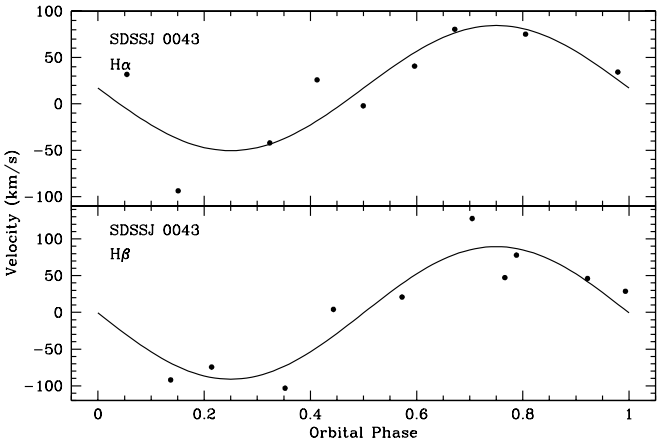

FIG. 10.—Velocity curve of SDSSJ 0043 with the best-fit sinusoids from Table 4.

3.5. *Systems Showing the Underlying Stars*

Generally, the systems with the lowest mass transfer rates have accretion disks that are so tenuous that they contribute little light in comparison to the primary and secondary stars. In these systems, the broad Balmer absorption lines from the white dwarf are observed flanking the emission lines from the disk. TiO bands from the secondary star can also be present, as well as an upturn in the flux longward of 7000 Å. In the SDSS spectra obtained during 2002, there are many more such systems present than in the previous 2 yr of data. The 15 systems showing one or both of the underlying stars include SDSSJ 0043, 0900, 0904+03, 0904+44, 0951, 1152 (BC UMa), 1249, 1302, 1324, 1501, 1610, 1702, 1705, 1711, and 2232. Three of these systems are the eclipsing objects discussed in § 3.2, since a disk viewed edge-on (i.e., high inclination) is not as luminous as a disk seen face-on (Warner 1987). It is notable that several of the white dwarfs in the systems showing prominent absorption lines have been shown to be pulsating during follow-up studies conducted by Woudt & Warner (2004) and Warner & Woudt (2004).

SDSSJ 0043: Using the emission lines of Hα and Hβ, our 2.7 hr of data suggest a period near 1.5 hr from Hα and near 1.2 hr from Hβ (Table 4). Since Hα is a stronger line and is not affected by the surrounding absorption of the higher Balmer series, it represents the best solution, but a longer time series of observations is needed to accurately pin down the period. Figure 10 shows the best-fit radial velocity curves for both lines.

SDSSJ 0900: This object is unusual in that it shows a prominent M star but does not show any evidence for the white dwarf. Either the white dwarf is very cool, the M star is evolved, or the accretion rate is relatively high in this system so that it obscures the white dwarf. The light curve shows a modulation of 2.6 hr (Fig. 11), whereas the radial velocity solution (Table 4 and Fig. 12) suggests the period is twice this value. The most logical interpretation is that the light curve is showing the ellipsoidal variation due to the prominent secondary.

SDSSJ 1249: While this object is listed in the catalog of Kilkenny et al. (1988) as a hot subdwarf, the SDSS spectrum clearly shows the presence of an M star. The Balmer lines all have narrow, strong emission-line cores. Thus, this system appears to have a hot star in close proximity to a highly irradiated M star. While there may not be mass transfer going on, this system may be a pre-CV or a system undergoing a time of low mass transfer.

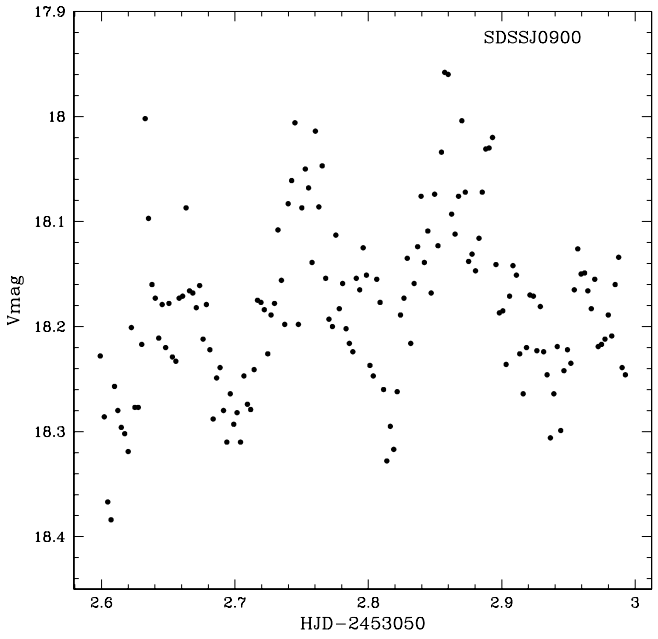

FIG. 11.—NOFS light curve of SDSSJ 0900 showing the 2.6 hr modulation. Integration times are 3 minutes, with 0.03 mag errors.

SDSSJ 1302: This system's spectrum resembles that of a symbiotic star (not strictly a CV), with a prominent M companion and very strong narrow emission lines with a recombination decrement. However, this object lacks the high-excitation lines (e.g., He II) typical of symbiotics. (See reviews of symbiotic stars in Corradi et al. 2003.)

3.6. *Undetermined Objects*

The object SDSSJ 1156 defies ready classification. While it has strong Balmer emission, the lines are very narrow for a CV and the continuum turns over in the blue. It also appears to have an emission line of He I λ5876 that is unusually strong. Since this object is quite faint, it could be an accreting system

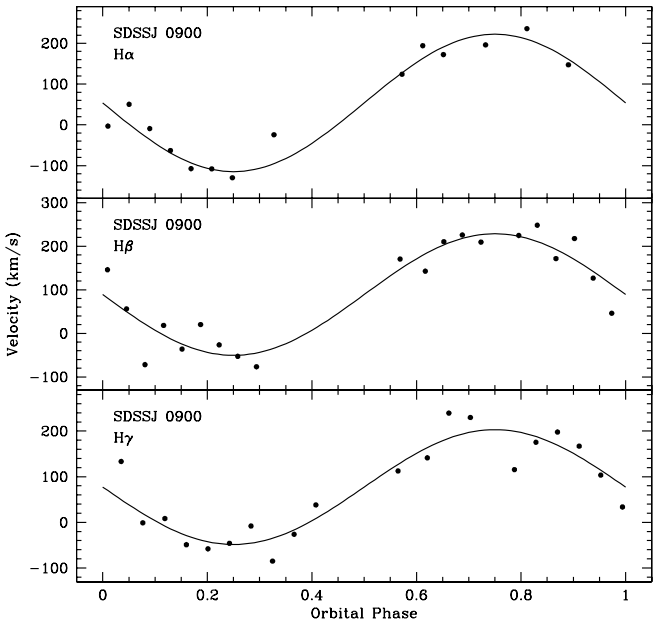

FIG. 12.—Radial velocity curves of SDSSJ 0900 with the best-fit sinusoids from Table 4. Note the period is twice that of the photometry.

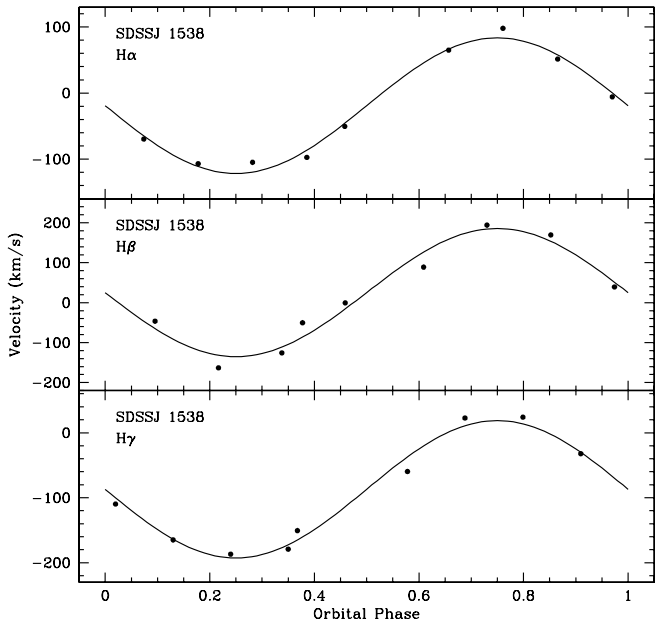

FIG. 13.—Radial velocity curves of SDSSJ 1538 with the best-fit sinusoids from Table 4.

in a low state, such as a polar. Further observations will be needed to sort out its correct identification.

APO spectra suggest a period near 1.6 hr for SDSSJ 1538 (Table 4 and Fig. 13). The spectral appearance (Fig. 1) and short period are typical for a normal dwarf nova. Long-term photometric monitoring can reveal if this system shows typical dwarf nova outbursts, and monitoring during an outburst can reveal if it shows the superhump phenomena typical of those systems with periods less than 2 hr (SU UMa systems).

3.7. *ROSAT Correlations*

Matching the coordinates of the CVs in Table 1 with the X-ray *ROSAT* All Sky Survey (RASS; Voges et al. 1999, 2000) reveals that five have X-ray detections (>2.5 σ) within the positional errors of the RASS. Table 5 presents the X-ray count rates for the five sources. The previously known dwarf nova KS UMa is included in this list. The low flux levels are typical for faint CVs with accretion disks. Surprisingly, none of the candidates for magnetic systems, which usually have larger X-ray fluxes than disk systems, appear in this list.

TABLE 5
ROSAT DETECTIONS

SDSSJ	*ROSAT*[a] (counts s^{-1})	Exp. (s)	RXS
0943.....	0.03 ± 0.01	544	J094327.7+520139
1020.....	0.12 ± 0.02	560	J102027.1+530439 = KS UMa
1132.....	0.025 ± 0.009	576	J113213.3+624903
1244.....	0.03 ± 0.01	533	J124424.5+613511
1538.....	0.07 ± 0.01	735	J153818.5+512348

[a] For a 2 keV bremsstrahlung spectrum, 1 count s^{-1} corresponds to a 0.1–2.4 keV flux of about 7×10^{-12} ergs cm^{-2} s^{-1}.

4. CONCLUSIONS

The 36 CVs described here, combined with the 64 from Papers I and II, provide substantial additions to the database of low-luminosity, short orbital period CVs that are postulated to compose the true population of CVs (Howell et al. 2001). While the overall detection rate (0.03 deg^{-2}) is comparable to that in Papers I and II, this latest set of CVs has fewer magnetic candidates (four) but many more systems (15) showing the underlying stars than in the past papers. Of the 12 systems with periods estimated (listed in Table 1), eight are less than 2 hr, three are in the period gap between 2 and 3 hr, and only one is above 3 hr. If the period estimates are confirmed and are representative of the rest of the group, the proportion of systems with short periods in the SDSS data will be larger than that from brighter surveys such as the Palomar-Green (Green et al. 1982; online Downes CV catalog gives periods) or the recent Hamburg Quasar Survey (Gänsicke et al. 2002). This would be consistent with the population models that predict most CVs should have evolved to short orbital periods and low mass transfer rates.

This sample highlights several interesting candidates for further study. Of the three eclipsing systems found, SDSSJ 1702 is especially important in that the secondary M1.5 star is evident, so that the masses may be determined with a large telescope. Further photometry of SDSSJ 0748 is needed to determine if it could be an IP. The exact nature of systems such as SDSSJ 1156, 1335, and 2102 remain to be explored. In addition, fitting of the underlying stars in the 15 systems that show them can reveal the temperatures and distances of this sample, yielding some estimate of age and heating effects from the ongoing accretion.

Funding for the creation and distribution of the SDSS Archive has been provided by the Alfred P. Sloan Foundation, the Participating Institutions, the National Aeronautics and Space Administration, the National Science Foundation, the U.S. Department of Energy, the Japanese Monbukagakusho, and the Max Planck Society. The SDSS Web site is http://www.sdss.org/. The SDSS is managed by the Astrophysical Research Consortium for the Participating Institutions. The Participating Institutions are the University of Chicago, Fermilab, the Institute for Advanced Study, the Japan Participation Group, Johns Hopkins University, Los Alamos National Laboratory, the Max-Planck-Institut für Astronomie, the Max-Planck-Institut für Astrophysik, New Mexico State University, the University of Pittsburgh, Princeton University, the US Naval Observatory, and the University of Washington. P. S., N. S., and S. H. acknowledge support from NSF grant AST 02-05875. Studies of magnetic stars and stellar systems at Steward Observatory is supported by the NSF through AST 97-30792.

REFERENCES

Abazajian, K., et al. 2003, AJ, 126, 2081 (DR1)
———. 2004, AJ, 128, 502 (DR2)
Bond, H. E., White, R. L., Becker, R. H., & O'Brien, M. S. 2002, PASP, 114, 1359
Corradi, R. L. M., Mikołajewska, J., & Mahoney, T. J., eds. 2003, ASP Conf. Ser. 303, Symbiotic Stars Probing Stellar Evolution (San Francisco: ASP)
Croom, S. M., Smith, R. J., Boyle, B. J., Shanks, T., Loaring, N. S., Miller, L., & Lewis, I. J. 2001, MNRAS, 322, L29
Fukugita, M., Ichikawa, T., Gunn, J. E., Doi, M., Shimasaku, K., & Schneider, D. P. 1996, AJ, 111, 1748
Gänsicke, B. T., Hagen, H.-J., & Engels, D. 2002, in ASP Conf. Ser. 261, The Physics of Cataclysmic Variables and Related Objects, ed. B. T. Gänsicke, K. Beuermann & K. Reinsch (San Francisco: ASP), 190

Green, R. F., Ferguson, D. H., Liebert, J., & Schmidt, M. 1982, PASP, 94, 560
Gunn, J. E., et al. 1998, AJ, 116, 3040
Hawley, S. L., et al. 2002, AJ, 123, 3409
Hogg, D. W., Finkbeiner, D. P., Schlegel, D. J., & Gunn, J. E. 2001, AJ, 122, 2129
Howell, S. B., Nelson, L. A., & Rappaport, S. 2001, ApJ, 550, 897
Jiang, X.-J., Engels, D., Wei, J.-Y., Tesch, F., & Hu, J.-Y. 2000, A&A, 362, 263
Kilkenny, D., Heber, U., & Drilling, J. S. 1988, South African Astron. Obs. Circ., No. 12
Lupton, R. H., Gunn, J. E., Ivezić, Ž., Knapp, G. R., Kent, S., & Yasuda, N. 2001, in ASP Conf. Ser. 238, Astronomical Data Analysis Software and Systems X, ed. F. R. Harnden, Jr., F. A. Primini, & H. E. Payne (San Francisco: ASP), 269
Lupton, R. H., Gunn, J. E., & Szalay, A. S. 1999, AJ, 118, 1406
Mukai, K., et al. 1990, MNRAS, 245, 385
Pier, J. R., Munn, J. A., Hindsley, R. B., Hennessy, G. S., Kent, S. M., Lupton, R. H., & Ivezić, Ž. 2003, AJ, 125, 1559
Reid, I. N., Hawley, S. L., & Gizis, J. E. 1995, AJ, 110, 1838
Shafter, A. W. 1983, ApJ, 267, 222
Smith, J. A., et al. 2002, AJ, 123, 2121
Stoughton, C., et al. 2002, AJ, 123, 485 (erratum 123, 3487)
Szkody, P., et al. 2002, AJ, 123, 430 (Paper I)
———. 2003a, ApJ, 583, 902
———. 2003b, AJ, 126, 1499 (Paper II)
Tramposch, J., et al. 2004, PASP, submitted
Usher, P. D., Mattson, D., & Warnock, A., III. 1982, ApJS, 48, 51
Voges, W., et al. 1999, A&A, 349, 389
———. 2000, IAU Circ. 7432
Warner, B. 1987, MNRAS, 227, 23
———. 1995, Cataclysmic Variable Stars (Cambridge: Cambridge Univ. Press)
Warner, B., & Woudt, P. A. 2004, in IAU Colloq. 193, Variable Stars in the Local Group, ed. D. W. Kurtz & K. R. Pollard (ASP Conf. Ser. 310) (San Francisco: ASP), 382
———. 2004, MNRAS, in press
Wickramasinghe, D. T., & Ferrario, L. 2000, PASP, 112, 873
Woudt, P. A., et al. 2004, in preparation
York, D. G., et al. 2000, AJ, 120, 1579